A MINIATURE OPTICAL EXTINCTION HEATED PROBE FOR FOG DROPLET MEASUREMENTS IN STEAM TURBINES

Ilias Bosdas
ibosdas@ethz.ch
Laboratory for Energy Conversion, Department of
Mechanical and Process Engineering,
ETH, 8092 Zurich, Switzerland
Anestis I. Kalfas
akalfas@auth.gr
Department of Mechanical Engineering, Aristotle
University of Thessaloniki, 54124
Thessaloniki, Greece

Michel Mansour
michel.mansour@lec.mavt.ethz.ch
Laboratory for Energy Conversion, Department of
Mechanical and Process Engineering,
ETH, 8092 Zurich, Switzerland
Reza S. Abhari
abhari@ethz.ch
Laboratory for Energy Conversion, Department of
Mechanical and Process Engineering,
ETH, 8092 Zurich, Switzerland

ABSTRACT

The knowledge of droplet size distribution and concentration allows us to calculate the wetness fraction and the isentropic turbine efficiency as well as to provide significant data for erosion modeling. For that purpose, a miniature optical extinction probe with a diameter of 9.4mm was designed, manufactured and tested. The probe is equipped with a heater, which maintains all optical components of the probe clean from any water contamination. In this paper the matrix inversion algorithm is presented in order to calculate the droplet diameter and concentration out of the spectral turbidity measurements. An ultrasonic atomizer was characterized in terms of droplet size and concentration with an established Phase Doppler Anemometry (PDA) system in order to have a reference spray environment for the proof of concept of the newly developed probe. Measurements were performed and results have shown a good agreement between the PDA technique and the optical extinction probe at various axial locations from the nozzle exit of the droplet generator.

NOMENCLATURE
Symbols

C	Concentration	$[droplets/cm^3]$
D	Diameter	$[m]$
E	Extinction coefficient	$[-]$
I	Light intensity	$[Watts/m^2]$
L	Distance	$[mm]$
m	Refractive index	$[-]$
N	Distribution	$[-]$
r	Radius	$[mm]$
u	Velocity	$[m/s]$
Y	Wetness mass fraction	$[\%]$

Greek symbols

α	Size parameter (Mie)	$[-]$
θ	Scattering angle	$[deg]$
λ	Wavelength	$[nm]$
τ	Turbidity	$[cm^{-1}]$
ϱ	density	$[kg/m^3]$

Subscripts

10	Arithmetic mean diameter
32	Sauter mean diameter
d	Droplet
m	Mass
M	Most frequent value in a data set
n	Number
o	Incident light intensity

Abbreviations

EMPA	Swiss Federal Laboratories for Materials Science & Technology
LEC	Laboratory for energy conversion
LP	Low-pressure steam turbine
OEP	Optical Extinction Probe
PDA	Phase Doppler Anemometry

INTRODUCTION

Fog droplet measurements in the last stages of low-pressure steam turbines are essential not only to quantify and assess the stage efficiency but also to understand the complex environment of the two-phase flow field. Coarse droplets are those that cause blade erosion at the tip of the last rotor, however many times fog droplets are responsible for the creation of large droplets through different generation mechanisms [1]. The most promising technique for measuring these small droplets in the submicron range is the optical extinction method as described by the Beer-Lambert law. This principle is used in the well known optical extinction probes, which are used in steam turbines since 1970s with some of the first attempts made by Walters et al. [2], Tatsuno et al. [3] and Young et al. [4]. The light extinction method is also used in references [5, 6] for droplet measurements in the last stages,

however, the probe tip diameters are limited to 20mm and a consequence the interaction with the flow field can be considered high. According to the literature review the smallest optical extinction probe was build by Schatz et al. as presented in [7, 8]. This probe has a tip diameter of 10mm and combines an optical and pneumatic part for the time averaged flow field measurements with the nulling technique. Since the surfaces of all probe types are prone to water contamination, the results of the optical extinction probes can be influenced by overestimating the turbidity. The current paper presents the design and development of the first version of an optical extinction probe with installed heating elements on a diameter of 9.4mm. The principal idea is to heat the probe tip in order to clean the optical components from water contamination and improve the results of the fog droplet measurements.

1 Optical extinction probe for fog water droplet measurements

In general, there are three sources of light intensity attenuation in the light beam direction: Diffraction, absorption and scattering. While diffraction and absorption are often negligible for spectral turbidity applications in fine water fogs, scattering is the dominant effect that causes a decrease in light intensity. Scattering can be described as the redirection of radiation out of the original direction of light propagation, usually due to interactions with molecules and particles. Besides the fundamental results of Mie theory regarding the mathematical description of light scattering, the Beer-Lambert law describes the essential equation for light transmission in a scattering medium [9].

1.1 Probe's operating principle

For the operating principle of the optical extinction probe only forward scattering is considered, therefore it is worth describing how the light intensity is linked to the extinction coefficient.

The extinction coefficient E describes how efficient the scattering process is, i.e. the higher E, the more light is scattered and therefore the attenuation in the propagation direction increases. Particle scattering is expressed in terms of cross section area and efficiency factors and the extinction coefficient E is defined as:

$$E = \frac{total\ flux\ scattered\ by\ the\ droplet}{flux\ geometrically\ incident\ on\ particle}$$

The extinction coefficient is calculated for spheres by Mie theory out of the fundamental Maxwell equations [9]. It can be considered as an optical property of the material: knowing the complex refractive index, and the diameter, E can be calculated as a function of wavelength, i.e. $E=E(\lambda,D,m)$. Setting the refractive index as

constant, since this quantity is not expected to change in the case of fog water droplet measurements, E can be represented as a surface plot. This is shown in Figure 1, where the extinction coefficient E is plotted for multiple wavelengths and various water droplet diameters.
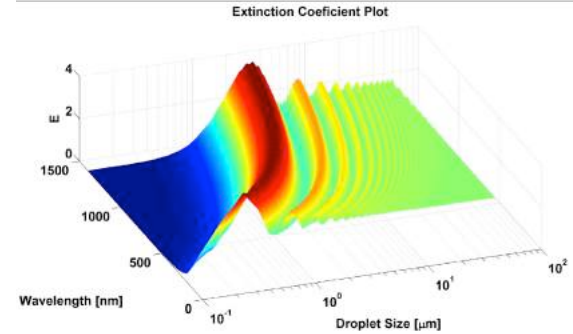

Figure 1: Surface plot of the extinction coefficient E for a constant refractive index (Water) as a function of wavelength and droplet diameter.

When light with initial intensity I_o passes through an absorbing and scattering medium, the intensity decreases along its path L following the Beer-Lambert law as expressed in Eq.(1-1). Therefore, the transmitted light I that leaves the control volume has a lower intensity. The Beer-Lambert Law provides the governing equation to calculate the transmission I/I_o in the forward direction.

$$I = I_o e^{-\tau \cdot L} \qquad (1\text{-}1)$$

For the derivation of the Beer-Lambert Law the following assumptions must be made:
- The droplets are evenly distributed in the considered volume (i.e. no concentration gradients)
- The droplets are treated as spheres
- The medium is non-absorbing
- Only independent single scattering occurs

At this point it must be emphasized, that the assumption of a non-absorbing medium in the case of water is reasonable, since the imaginary part of its refractive index is very small and in particular at 20°C is $1.33+1.67 \times 10^{-8}$i, hence the complex part is negligible compared to the real part. The intensity reduction of the transmitted light I is a function of the distance L and turbidity τ.

The turbidity τ used in Eq.(1-1) can be calculated using Eq.(1-2) assuming a droplet distribution of N(D) and applying the extinction coefficient E for the water medium as presented previously.

$$\tau = \int_0^\infty \frac{\pi}{4} D^2 N(D) E_{(D,\lambda,m)} dD \qquad (1\text{-}2)$$

When Eq.(1-1) is used, the relative attenuation I/I_o is measured for multiple wavelengths with the help of a spectrometer. These set of equations provide the information to convert the spectral transmission

signal into droplet size distribution and concentration, which are then extracted in the post-processing steps after the measurements. In practice, the spectral transmission is measured with a white light (i.e 400 to 800nm), which is collimated by a lens. As shown in Figure 2, the light from a white source is guided through an optical fiber (inlet fiber) to the probe tip. A collimating lens guides the light to an open aperture where the fog droplets can travel through. When the present medium has a scattering behavior, such as a droplet laden flow, the light gets extinct along its path, in this case the 5mm gap. The illuminated droplets scatter the incident light and thus, reducing the light intensity in the forward direction. At the end of the measurement volume, the collimated beam is reflected back with a mirror, causing the rays to undergo the same scattering process again. The light is then focused back into another fiber optic by the same lens and finally, the spectral intensity of the signal is measured with the spectrometer. In order to measure the relative spectral extinction, the measurements must be performed with and without the droplets so as to obtain the ratio of I/I_o.
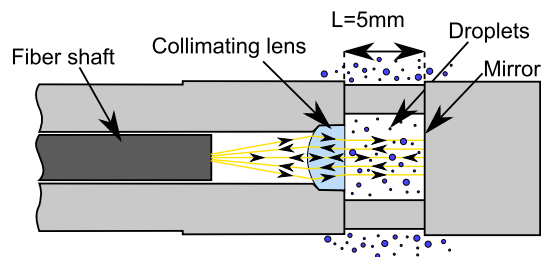

Figure 2: Operating principle of the optical extinction probe: A collimated light beam is attenuated by $e^{-2L\tau(\lambda)}$ across the 2L length. This is measured by generating the ratio of the reference spectrum I_o without droplets and the attenuated spectrum I with droplets.

1.2 The optical extinction probe

The final design of the optical extinction probe is shown in Figure 3.a. In order to avoid any water contamination and beam deflection a high power density heater was installed in the probe tip. The purging approach was not considered as a viable solution since the purging flow would disturb the flow entering the sample volume of the probe and therefore the influence the results. During the design process, an effort was made to maintain the tip diameter as small as possible in order to minimize any interaction with the surrounding flow field. The result is a compact probe tip with a diameter of 9.4mm and a miniature heater with a heating power density of 38W/cm². Additional thermocouples were installed in order to control and monitor the heater performance through a PID controller. A cross section of the probe tip, to the point where the heating elements are apparent, is

shown in Figure 3.b. Both the collimating lens and mirror are heated directly from the heater due to its high proximity to the optical components. This is achieved with a thin wire with high specific resistance wrapped around a thermally conductive substrate. Although one single heating wire was used, the heater can be split up into two parts: The heating wires in the mirror and lens region as indicated in Figure 3.b. The wires start from the mirror region (top) and pass to the lens region through the two cylindrical rods indicating the complexity of the probe tip in these miniature dimensions.
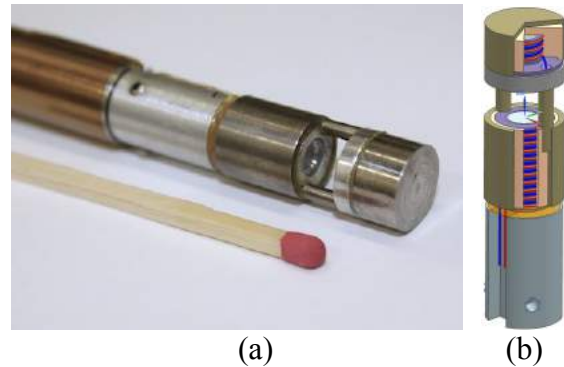

(a)   (b)

Figure 3: The optical extinction probe tip (a) and a schematic of the tip with the heating wires in a double helix configuration marked with red and blue (b).

1.3 Experimental quantification of heating power distribution across the probe tip

In order to test the performance of the heater and its ability to maintain the optical components of the probe clean from any water contamination, the probe was tested under representative steam flow conditions in a freejet facility as well as in a steam generator. The flow conditions are Nusselt number representative of the last stage of a low pressure steam turbine. At 80% of the blade span the typical conditions, which were used, are 0.35 Mach number, 44°C and static pressure of around 8kPa. Three different conditions were tested were the Nusselt number was varied with the maximum value of Nu=108 when the wetness fraction of 10% was used in the calculations. Two thermocouples were installed on the probe tip, one on the center of the collimating lens and one on the center of the mirror as these components are presented in Figure 2. As shown in Figure 4, a minimum temperature overheat of 20°C is achieved in all test cases for both the mirror as well as the lens. The mirror though shows always lower overheat temperatures of about 50% less compared to the collimating lens. This is explained by the lower power density, which is installed in the upper part of the probe tip as shown in the schematic of Figure 3.b
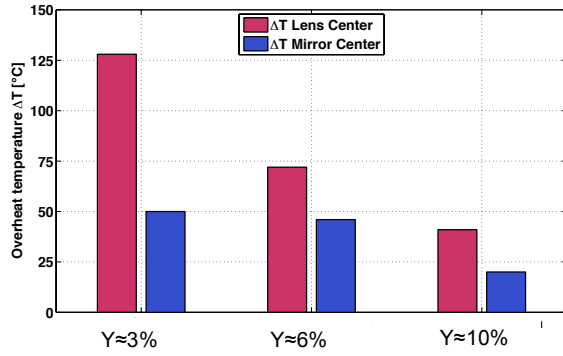
Figure 4: Results of the heater performance tests at three representative flow conditions from the last stage of a low pressure steam turbine. The absolute temperature of the heating elements was always set to 250°C.

1.4 Numerical approaches to process the optical extinction data

The calculation of the droplet concentration distribution and the resulting wetness fraction, from the optical extinction probe results, is not a trivial process. Regarding the theoretical background (Beer-Lambert Law and Mie theory) the desired quantities can be related to the spectral light extinction described in a Fredholm integral equation. The governing equation for light transmission according to the Beer-Lambert law for a specific wavelength λ_i and constant refractive index m is described with Eq.(1-3).

$$\frac{1}{L}\ln\left(\frac{I_o}{I}\right)\bigg|_{\lambda=\lambda_i} = \int_0^\infty \frac{\pi}{4}D^2 N(D)E(D,\lambda_i)dD \qquad (1\text{-}3)$$

This integral equation can be characterized as a Fredholm integral equation of the first kind [10, 11] with the following form:

$$g(y) = \int_a^b K(x,y)f(x)dx \qquad (1\text{-}4)$$

with the kernel K(x,y), the measured g(y) and the desired function f(x). Several different methods exist in order to solve equation Eq.(1-3) or Eq.(1-4) for N(D) or f(x) respectively [1, 11]. Two different methods were used in order to solve the spectral turbidity equation and obtain the droplet diameter and concentration. The first one is the matrix inversion approach and the second is the curve fitting approach. The two data processing algorithms for the extinction probe were developed in MATLAB environment. For compactness of this paper only the matrix inversion approach is described since it shows the best results. A sensitivity to white noise was performed for both processing routines, due to the fact that the Fredholm integral equations are extremely sensitive to noise. Both approaches show a good robustness for the low levels of simulated noise (~1%), resulting in a relative error of less than 10% on the

Sauter mean diameter D_{32}, concentration C_n and wetness fraction Y. However when the noise increases to 10% the error can reach up to 50% depending of the case. As a conclusion, the power of the white light source, which is used for the optical extinction probe and presented in the following paragraphs, should be as high as the optical components can resist in order to obtain the maximum signal to noise ratio.

Matrix inversion approach

The main advantage of this approach is that it does not require an a priori knowledge of the droplet distribution. It is only taken into account, that the distribution is smooth, non-negative and zero at the outer boundaries. In a first step, the integral is approximated with a numerical quadrature. Several numerical approaches exit to calculate a general integral in the form of Eq.(1-5).

$$I = \int_a^b f(x)dx \qquad (1\text{-}5)$$

The Gaussian quadrature is a numerical integration method with a maximal accuracy for the given discretization points. The seek out of the best quadrature formula is less relevant, since the error induced due to the quadrature approximation is very little. Nevertheless, the Gaussian quadrature provides the same accuracy as a simple quadrature formula, such as the trapezoidal method but with less discretization points M. It transforms the integral into a weighted sum of functions evaluation points to

$$I = \sum_{j=0}^M w_j f(x_j) \qquad (1\text{-}6)$$

where M is the number of desired points and w_j is the nonzero weighting factor for the function evaluation $f(x_j)$. Once the number of points M is set, the weightings can be calculated according to Eq.(1-7),

$$w_j = \frac{b-a}{2}\int_{-1}^1 \prod_{\substack{k=1 \\ k\neq j}}^M \left(\frac{u-u_k}{u_j-u_k}\right)^2 du > 0; j=1,2,3,...,M$$

$$(1\text{-}7)$$

where u_j and u_k are the zeros of the j-th or k-th Legendre polynomial respectively. The evaluation points of the function f(x) are:

$$x_j = \frac{b+a}{2} + \frac{b-a}{2}u_j \qquad (1\text{-}8)$$

It is worth noting that the number of points M defines the resolution of the integral and can be set by the user. Nevertheless, M cannot be set arbitrary high. The degree of accuracy is 2M−1 (meaning that a polynomial with degree 2M−1 can be calculated exactly). Thus, the Gaussian quadrature is a powerful instrument, but it must be emphasized

that the number of points M, which defines the resolution, cannot be arbitrary large. The reason is that the larger the M value is, the higher the frequencies, which are introduced. This causes unstable or oscillating solutions. Nevertheless, the principle of this procedure is the accurate approximation of a continuous integral with a sum of M summands. Adapting this quadrature approximation on Eq.(1-3), the spectral transmission equation has the following form:

$$\frac{1}{L}\ln\left(\frac{I_o}{I}\right)\Bigg|_{\lambda=\lambda_i} = \sum_{j=0}^{M} w_j \frac{\pi}{4} D_j^2 E(D_j,\lambda_i)N(D_j) \quad (1\text{-}9)$$

Finally, the equation can be written in a matrix form according to Eq. (1-10).

$$\vec{g} = A \cdot \vec{f} \quad (1\text{-}10)$$

The mathematics allows the solution of Eq.(1-10) by inverting the matrix A. However, this leads to catastrophic results for the solution of x, such as unwanted oscillations or negative, not feasible solutions [12]. The physical nature of this problem sets an a priori constrain to the solution vector f, i.e. f must be non-negative and smooth. One approach to overcome this effect of unstable solutions is to induce controlled smoothing to the solution. This technique is proposed in [12] and it applied by to particle sizing applications from Walters in [11]. As a result the smoothing matrix H is introduced to the regularized non negative least square problem. The equation that has to be solved is now expressed with Eq.(1-11).

$$f = \left(A'A + \gamma H\right)^{-1} A'g \quad (1\text{-}11)$$

However, it is often the case, where certain elements of f are negative, since Eq.(1-11) has no restriction on the sign of f. To avoid such an unfeasible solution, the problem described above is solved with a non negative least squares (NNLSQ) solution. In terms of mathematics, the problem can be expressed with Eq.(1-12).

$$\min\left\{\|Af - g\|^2 + \gamma f'Hf\right\}, with\, f_i \geq 0 \quad (1\text{-}12)$$

To end up with a feasible solution vector for the concentration f, the smoothing parameter γ must be chosen as small as possible, since it is an artificial perturbation of the original physical equation.

The determination of a suitable smoothing parameter is not a straightforward procedure since the value of γ might cover up several orders of magnitude. A common task to solve such a regularization problem is presented by Su et al. in [13], often referred as regularization problem. Such problems can be solved with the L-curve approach. As the name implies, the name of the L-curve is inferred from its shape, which is monotonically decreasing and has the shape of the letter "L" as shown in Figure 6. The higher the smoothing parameter γ is, the less accurate the results are and vice versa. Hence, when γ is very small the solution

is very accurate but on the other hand, f shows large oscillations. The optimum solution is on the corner of the L shape where both smoothing and accuracy are optimized.

In order to test the inversion algorithm and the smoothing parameter γ, three well-known artificial distributions were used to calculate the spectral turbidity vector g as presented in Eq.(1-10). These distributions are presented in Figure 5. In addition, normal distributed noise was added to g with a mean value of 0%, 0.2%, 0.5%, 1%, 5% and 10% respectively. In a second step the system matrix A and the smoothing matrix H were set up for 1nm equidistant values of λ in the range of 400nm≤λ≤800nm. Finally, the distribution is recalculated by solving Eq.(1-12) and compared with the original distribution. The goal of this task was to assess the noise effects on the inversion process. As shown in Figure 5, Case 1 is a broad log-normal distribution with a probability peak in the lower diameter region. Case 2 is a narrow normal distribution in the upper diameter range and case 3 a bi-modal distribution with two probability peaks. The way to get a solution for a specific case can be described in the following steps:

1. Calculate the L-curve for several values of γ.
2. Determine the optimal value of γ by detecting the corner point of the L-curve (this step is illustrated in Figure 7 for case 3 with 0.5% noise).
3. Solve constrained non-negative least square problem described in Eq.(1-12) with the optimal value of γ.
4. Calculate key numbers: Sauter mean diameter, wetness fraction and concentration and compare it with the theoretical value.
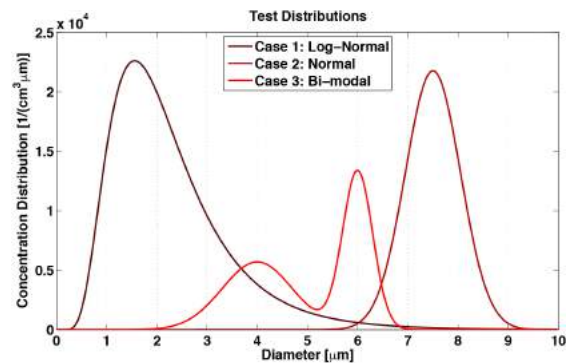

Figure 5: Test distributions for matrix inversion approach

A typical result of this algorithm test is presented in Figure 7 and Figure 8 with the example of 0.5% noise for case 3. For compactness of this paper results only from this distribution are presented since this is the most complicated one for the code to process it.
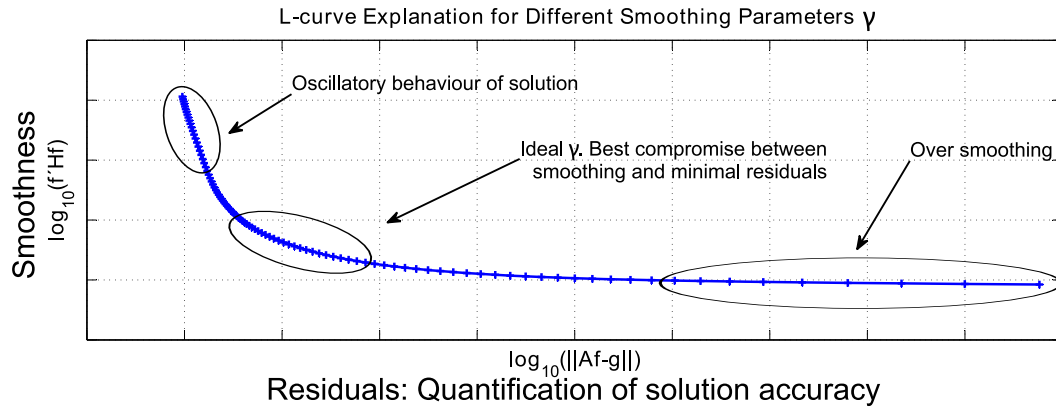
5

Figure 6: The of the L-curve is the optimum solution for γ. It represents the best compromise between smoothness and accuracy.
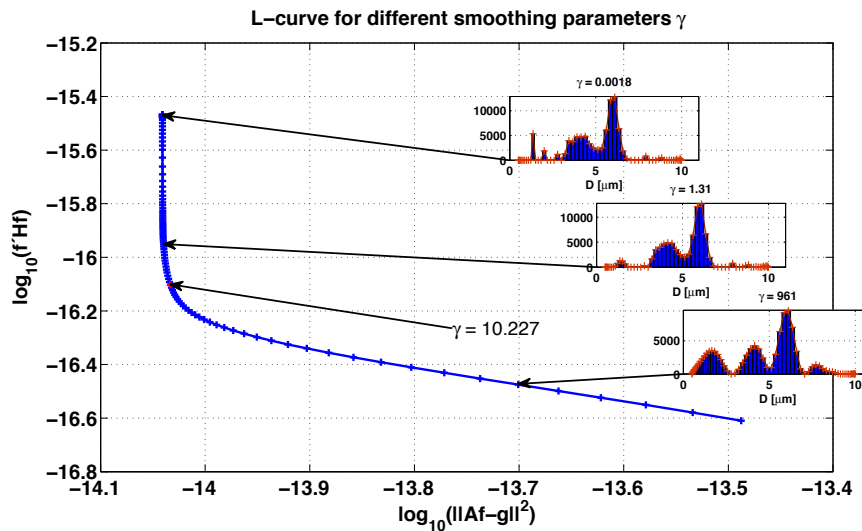

Figure 7: L-Curve with 0.5% noise on the turbidity τ: The y-coordinates of the points in this logarithmic plot represent $\log_{10}(f^{'}Hf)$ and the x-coordinate is assigned with the residuals for different values of γ. As indicated with the arrow an ideal value for γ of 10.227 was calculated with the code.

When the system matrices A, H, and g are calculated, the smoothing parameter γ can be optimized by using the L-curve approach. In the next step, the solution f is calculated with the optimized γ, which is compared with the predefined initial distribution N(D) in this case with the bi-modal distribution as shown in Figure 5. The comparison between the test distribution and the results from the developed inverse algorithm for this case can be seen in Figure 8. The input distribution to the code is shown with the dashed grey line and the output of the inverse algorithm is the histogram plotted in blue. As shown in Figure 8, there is a very good agreement between the two distributions for this noise level that indicates the accuracy of the code. The difference in Sauter mean diameter and concentration is 1.8% and 3.1% respectively. In addition, sensitivity tests on the results of the inversion matrix algorithm to a Gaussian noise are shown in Figure 9 for the bi-modal distribution. When the noise is set to 0% the algorithm can produce almost exactly the predefined distribution. The algorithm can resolve

the distribution for noise level up to 0.5% with an accuracy of 6% in D_{32}, D_M and concentration however at a noise level above 1% an additional peak starts to appear in the solution.
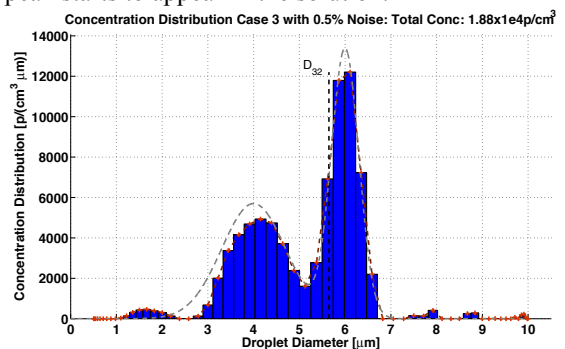

Figure 8: Solution of the matrix inversion algorithm for case 3 with 0.5% noise. With an ideal smoothing factor γ obtained from Figure 6. For the current results the non-negative least squares algorithm was used Eq.(1-12)
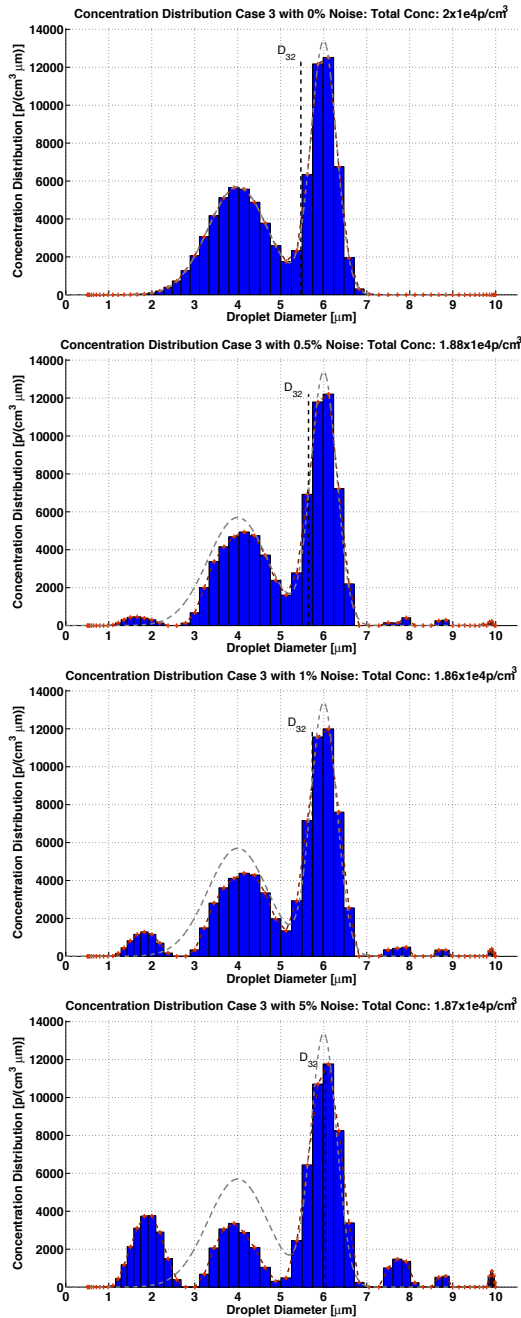
Figure 9: Solution of the matrix inversion algorithm for case 3 (Bi-modal distribution) with different Gaussian noise levels (0%, 0.5%, 1% and 5%)

2 Proof of concept tests with the optical extinction probe

2.1 Fog droplet spray characterization using the PDA measurement technique

The lack of calibration procedure for the optical extinction probe is the main challenge when assessing the obtained results of the droplet size distribution and concentration. Since there is no calibration procedure for the extinction technique and the results are calculated from the solution of Beer-Lambert law, the accuracy of the whole measurement chain of the new measurement system had to be assessed. Pre-characterized particle samples with well known optical properties can be used such as glass beads or polystyrene micro spheres [14]. However, these calibration approaches require a correction procedure taking into account the different optical properties of water compared to glass.

In order to assess the quality of the results with the new probe, a direct comparison with reference measurements was made. Five different sprays from five different spray generators were characterized in terms of droplet size distribution, speed and concentration at different locations on the spray propagation path with a Phase Doppler Anemometry (PDA) system developed in the Swiss Federal Laboratories for Materials Science and Technology (EMPA) [15]. However, for compactness of the paper only the results from an ultrasonic atomizer are presented in this paper. Ultrasonic nozzle atomizers are a type of spray nozzle that uses high frequency sound waves produced by piezoelectric transducers acting upon the nozzle tip that will create capillary waves in a liquid film. Once the amplitude of the capillary waves reach a critical height they become too tall to support themselves and tiny droplets fall off the tip of each wave resulting in atomization [16]. As a consequence, droplets in the micro range diameter are generated.

The Phase Doppler Anemometry (PDA) principle is an optical method to measure droplet sizes and velocity components at a certain location. Two monochromatic lasers are used: A green laser (λ=514.5nm) for the size determination and the main velocity component and a blue laser (λ=488nm) for the lateral velocity. The laser power intensity was 500mW. The collimated laser beams are both separated and one beam is phase shifted with a Bragg cell. When focusing back the splitted laser beams in the measurement volume, an additive-destructive interference pattern is created. These layers are called fringes and shown in Figure 10.
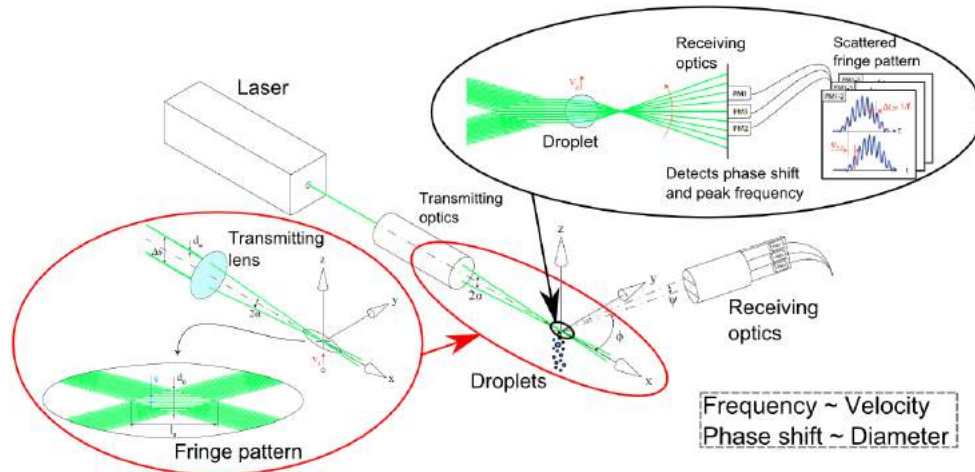
Figure 10: Determination of droplet speed and size using Phase Doppler Anemometry (PDA). The peak frequency is used to calculate the speed and the phase shift is used to calculate the droplet size [15, 17].

When a droplet crosses the measurement volume, the light of the fringe pattern is being scattered and detected from the receiving optics. The receiving optics are placed at the Brewster angle of 70° where the first diffraction mode is dominant and the detected fringe scattering pattern has an optimal quality to determine the frequency and phase shift. The droplet velocity can be determined by detecting the frequency of the peaks in the fringe signal, which is related to the velocity. On the other hand, the droplet size is measured by evaluating the phase shift of the whole scattered fringe pattern [17]. The measurement technique is illustrated with a schematic in Figure 10.

The spray from the ultrasonic atomizer was characterized in three different axial locations on its center axis as shown in Figure 11. Figure 11.a shows the actual measurement set up, with the PDA system. The ultrasonic atomizer is installed, such as that the measurement volume of the PDA is at the center of the spray at the desired distance from the nozzle exit. Finally, the scattering pattern is detected with the receiving optics located at the right side of Figure 11.a. Figure 11.b shows a schematic with the three measurement locations at the nozzle exit of the ultrasonic spray atomizer. The Sauter mean diameter D_{32} in [μm], mean diameter D_{10} in [μm], mode diameter D_M in [μm], wetness fraction Y in [%] and concentration C_n in [p/cm^3] are obtained from the PDA measurements. In addition, the PDA system provides information about the velocity components of the spray.
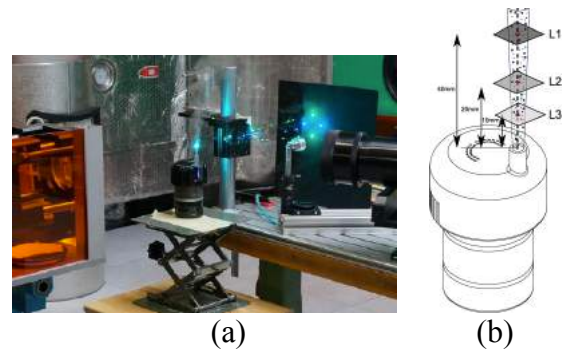

(a)　　　　　(b)

Figure 11: Experimental set up with the ultrasonic atomizer. The laser is focused with a lens (left), the measurement volume is at the spray center, on the right the receiving optics can be seen (a). PDA Measurement locations for the tested spray, L1, L2 and L3 (b).

2.2 Diameter and concentration results

The overall results for the three axial distance locations downstream of the exit nozzle are presented in Table 1.

Table 1: Ultrasonic atomizer results from three axial distance locations downstream of exit nozzle.

Distance L [mm]	D_{32} [μm]	D_M [μm]	Y [%]	C_n 10^3[p/cm^3]
10	9.4 ±4.7%	4.1 ±16%	2.8 ±19%	17.9 ±36%
20	9.2 ±0.7%	3.5 ±4%	3.1 ±12%	20.6 ±37%
40	10.5 ±5.1%	3.4 ±8.8%	3.8 ±13%	19.7 ±38%

3 Optical extinction probe results in comparison with PDA using an ultrasonic atomizer

3.1 Measurement set up

In this paragraph the results of the optical extinction probe from the measurements with the ultrasonic atomizer are presented. The spray was measured at three different axial locations (L1 to L3) representative of the measurements performed with the PDA system. A schematic of the measurement setup is shown in Figure 12. The optical extinction probe is powered with a 240W Volpi Intralux 6000-1 white light source to measure the spectral attenuation. For the spectral analysis of the transmission signal a HR2000+ spectrometer from Ocean Optics is used. In order to operate the spectrometer at maximum signal output, but below the 14Bit saturation limit of 214 photon counts, an adjustable in-line attenuator was used. This attenuator is a custom made adjustable pinhole. The aperture can be adjusted manually in order to tune the reflected light signal that is obtained with the probe. The probe measurement locations were at the same axial distances from the nozzle exit as the one with the PDA system. The positioning of the probe tip relative to the ultrasonic atomizer was controlled with linear translators with an accuracy of ±5μm.
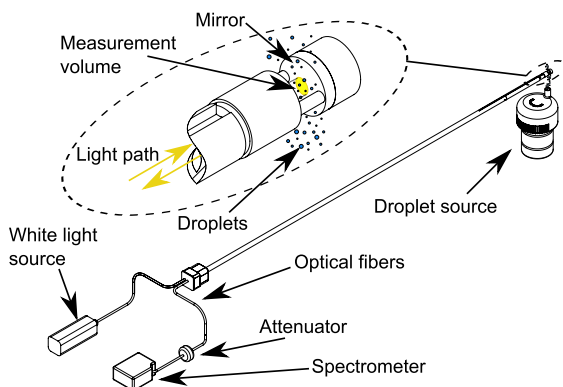

Figure 12: Measurement set-up schematic with the optical extinction probe and the droplet source (ultrasonic atomizer). The probe is connected to a white light source and the attenuated light signal is measured with a spectrometer.

3.2 Results and discussion

The optical extinction probe results as well as the PDA system results at 10mm, 20mm, and 40mm downstream from the atomizer's nozzle are presented in Figure 13, Figure 14 and Figure 15 respectively. As shown in Figure 13, Figure 14 and Figure 15, the maximum deviation in D_{32}, D_{10} and D_M diameter is less than 2.5μm in comparison with the reference case (PDA) for all distances. In particular, the larger discrepancies are found in the Sauter mean diameter, D_{32}, for all test cases. This is

because when the Sauter mean diameter is used for the calculations, the volume of the particle is taken into account and therefore large droplets have a greater impact on the calculations. Since the optical extinction probe has a measurement range up to 8 to 10 μm, depending on the white source spectrum, large droplets present in the spray are not detected and therefore the Sauter mean diameter is underestimated. This is shown as well in Figure 16 with the normalized droplet distribution for the case of 40mm downstream from the nozzle exit. In this plot the concentration can be decoupled from the results by normalizing the concentration distribution. The measurements with the PDA system indicate droplets up to 18μm in diameter. The significant portion between 10 and 18μm in diameter sets the Sauter mean diameter to a larger value in the PDA results compared to the OEP probe. Regarding the average and the most frequent values of the diameters the deviation between the two measurement techniques is below 1.2μm for all test cases. This is a very good agreement between the two techniques considering the wide range of droplets produced by the ultrasonic atomizer.
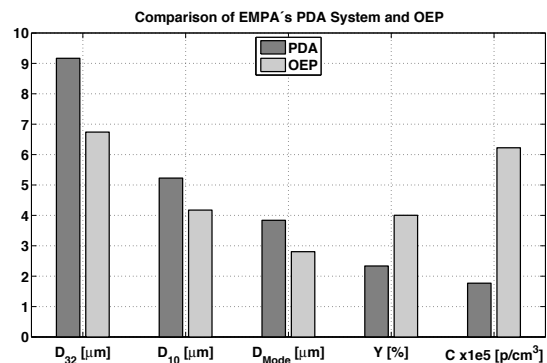

Figure 13: Results obtained with the optical extinction probe (OEP) and the PDA measurements with the ultrasonic atomizer at 10mm distance from the nozzle exit.
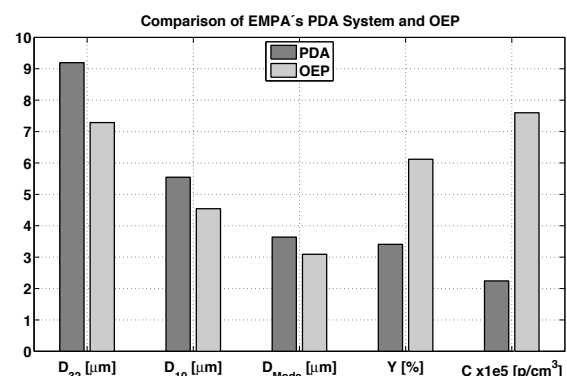

Figure 14: Results obtained with the optical extinction probe (OEP) and the PDA measurements with the ultrasonic atomizer at 20mm distance from the nozzle exit.
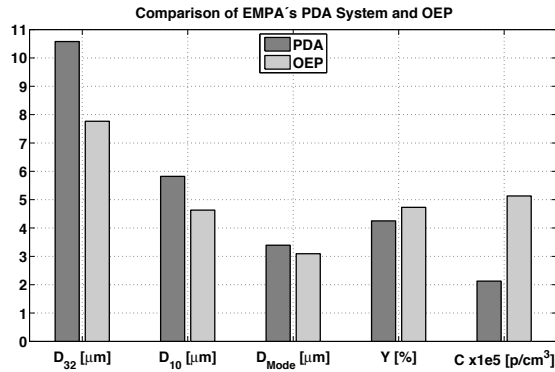
Figure 15: Results obtained with the optical extinction probe (OEP) and the PDA measurements with the ultrasonic atomizer at 40mm distance from the nozzle exit.
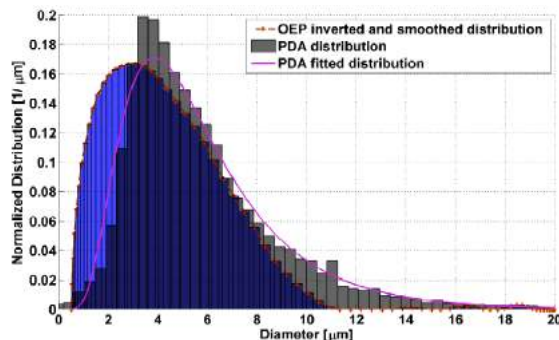

Figure 16: Normalized distribution diameter from the optical extinction probe (OEP) and the PDA measurements at 40mm from the nozzle exit of the ultrasonic atomizer.

Regarding the concentration and wetness fraction measurements, the results from the optical extinction probe are overestimated in all cases (L1, L2 and L3) when compared with the PDA results. The difference between the two techniques is roughly a factor of 3 for the three axial distances but in same the order of magnitude. This is important since the concentration values, which are found in the last stages of a steam turbine, are very high ($>10^6 p/cm^3$) [5] and thus the relative error is reduced. The main reason for this discrepancy is, that the PDA system uses a different measurement technique than the probe. The PDA system counts every droplet size by detecting the phase shift in the scattered fringe pattern as shown in Figure 10. However, the PDA processing code ignores droplets that are not spherical or multiple droplets in the sample volume at the same time instant. In addition, when a droplet is too small to create a detectable scattering pattern by the system, it is also ignored. As a result, the resolution of the system is reduced significantly when $D_d<4\mu m$. On the other hand, the optical extinction probe detects every droplet present in its sample volume, because each droplet scatters light by its nature and therefore has its contribution to the light extinction when it is exposed to the light beam. Therefore in

this case, it is believed that the deviation is due to the different detectable droplet range between the two measurement techniques.

4   Summary and conclusions

An optical extinction probe to measure the fog water droplets in the range of 0.2 to 10μm in diameter was successfully developed, designed, manufactured and tested. Although this is a well-known and established technique since the 1970s, as far as the authors are concerned this probe has the smallest size ever reported in the open literature. The probe tip diameter is 9.4mm and a high-power density heater is installed to prevent water contamination on its optical components. Two data processing algorithms for the extinction probe were developed in MATLAB environment. The matrix inversion algorithm is presented in the current paper since it is shows the best results in terms of accuracy for various noise levels.

In order to have a reference spray environment for the proof of concept of the newly developed probe, a Phase Doppler Anemometry (PDA) system, was used to quantify the spray from an ultrasonic atomizer at three axial locations downstream from the nozzle exit. The same measurements were performed with the optical extinction probe and the results between the two techniques were compared for the three locations from the nozzle exit. The maximum deviation between the PDA and the extinction probe was less than 2.5μm and 1.2μm for the Sauter mean (D_{32}) and most frequent diameter (D_M) respectively. In addition the mean absolute deviation for the logarithmic (log_{10}) concentration is less than 12%. The relatively large deviation in the concentration calculations can be explained with the different measurement principle techniques that the two instruments are applying.

REFERENCES
[1]   Moore, M. J. and Sieverding, C. H., *Two-phase steam flow in turbines and separators : theory - instrumentation - engineering*: Washington & London: Hemisphere New York a.o.: McGraw-Hill, 1976.

[2]   Walters, P. and Skingley, P., 1979, "An optical instrument for measuring the wetness fraction and droplet size of wet

steam flows in LP turbines," *Proc. Inst. Mech. Eng., Part C,* 141(79), pp. 337-348.

[3] Tatsuno, K. and Nagao, S., 1986, "Water Droplet Size Measurements in an Experimental Steam Turbine Using an Optical Fiber Droplet Sizer," *Journal of Heat Transfer,* 108(4), pp. 939-945.

[4] Young, J. B., Yau, K. K., and Walters, P. T., 1988, "Fog Droplet Deposition and Coarse Water Formation in Low-Pressure Steam Turbines: A Combined Experimental and Theoretical Analysis," *Journal of Turbomachinery,* 110(2), pp. 163-172.

[5] Cai, X., Ning, T., Niu, F., Wu, G., and Song, Y., 2009, "Investigation of wet steam flow in a 300 MW direct air-cooling steam turbine. Part 1: Measurement principles, probe, and wetness," *Proceedings of the Institution of Mechanical Engineers, Part A: Journal of Power and Energy,* 223(5), pp. 625-634.

[6] Hayashi, K., Shiraiwa, H., Yamada, H., Nakano, S., and Tsubouchi, K., "150 kW Class Two-Stage Radial Inflow Condensing Steam Turbine System," presented at the Volume 4: Cycle Innovations; Fans and Blowers; Industrial and Cogeneration; Manufacturing Materials and Metallurgy; Marine; Oil and Gas Applications, Vancouver, Canada, 2011, GT2011-46192.

[7] Schatz, M. and Casey, M., 2007, "Design and testing of a new miniature combined optical/pneumatic wedge probe for the measurement of steam wetness," *AIP Conference Proceedings,* 914(1), pp. 464-479.

[8] Eberle, T., Schatz, M., Starzmann, J., Grübel, M., and Casey, M., 2014, "Experimental study of the effects of temperature variation on droplet size and wetness fraction in a low-pressure model steam turbine," *Proceedings of the Institution of Mechanical Engineers, Part A: Journal of Power and Energy,* 228(1), pp. 97-106.

[9] Hulst, H. C. v. d., *Light scattering by small particles*, [Dover ed.] edition.: New York, N.Y. : Dover, 1981.

[10] Twomey, S., *Introduction to the mathematics of inversion in remote sensing and indirect measurements* vol. 3: Amsterdam [etc.] : Elsevier, 1977.

[11] Walters, P. T., 1980, "Practical applications of inverting spectral turbidity data to provide aerosol size distributions," *Applied Optics,* 19(14), pp. 2353-2365.

[12] Twomey, S., 1963, "On the Numerical Solution of Fredholm Integral Equations of the First Kind by the Inversion of the Linear System Produced by Quadrature," *J. ACM,* 10(1), pp. 97-101.

[13] Su, M., Xu, F., Cai, X., Ren, K., and Shen, J., 2007, "Optimization of regularization parameter of inversion in particle sizing using light extinction method," *China Particuology,* 5(4), pp. 295-299.

[14] Korolev, A., Shashkov, A., and Barker, H., 2013, "Calibrations and Performance of the Airborne Cloud Extinction Probe," *Journal of Atmospheric and Oceanic Technology,* 31(2), pp. 326-345.

[15] Kammermann, T., 2013,"Droplet characterization of HFO sprays by means of PDA," Master Thesis LAV, ETH Zurich.

[16] Lang, R. J., 1962, "Ultrasonic Atomization of Liquids," *The Journal of the Acoustical Society of America,* 34(1), pp. 6-8.

[17] Schneider, B., Hermann, K., and Obrecht, P., *Diagnostics in experimental combustion research*: LAV lecture series, ETH Zurich, 2013.